A study of multi-trapping of tapered-tip single fiber optical tweezers*

Liang Pei-Bo(梁佩博), Lei Jiao-Jie(雷皎洁), Liu Zhi-Hai(刘志海)†, Zhang Yu(张 羽), and Yuan Li-Bo(苑立波)

Key Laboratory of Fiber Integrated Optics, School of Science, Harbin Engineering University, Harbin 150001, *China*

(Received 29 October 2013; revised manuscript received 18 February 2014; published online 10 June 2014)

We develop a pair of tapered-tip single fiber optical tweezers, and study its multi-trapping characteristic. The finite difference time domain method is employed to simulate the trapping force characteristic of this pair of single fiber optical tweezers, and the results show that the number of trapped particles depends on the refractive index and the size of the particles. The trapping force of this pair of tapered-tip single fiber optical tweezers is calibrated by the experimental method, and the experimental results are consistent with the theoretical calculation results. The multi-trapping capability realized by the tapered-tip single fiber optical tweezers will be practical and useful for applications in biomedical research fields.

Keywords: optical trapping, microstructures and particles

PACS: 87.80.Cc, 42.50.Wk **DOI:** 10.1088/1674-1056/23/8/088702

1. Introduction

Optical tweezers (OTs) have been widely applied to the noninvasive manipulation of a variety of biological specimens[1–5] including viruses, bacteria, cells, and subcellular organisms in biology and biophysics research fields since they were invented by Ashkin *et al*. in 1986.[6] When the light from OTs is incident and deflected by the surface of an object, optical forces will be produced and exerted on the object due to the photon momentum change. Besides the biological field, OTs also open up new possibilities for handling areas revolutionized by microscopic particles, such as atomic physics,[7–9] chemistry,[10,11] and micro-electro-mechanical systems (MEMS);[12] even the study of the optical trapping itself has resulted in the advent of interesting new physics.[13,14]

Traditionally, optical trapping is achieved by traditional lens OTs, but the bulky structure and high cost restrict their applications in several environments, so optical fiber tweezers came into being. The early fiber OTs employed two or more optical fibers guiding light beams to build a large enough light field intensity gradient distribution for trapping,[15,16] which needs multi-high-precision micro-manipulators to control multi-optical fibers, so the cost of multi-optical fiber tweezers is still too high. Then, on the basis of fiber-end micromachining technology development, Taylor and Hnatovsky achieved the three-dimensional (3D) trap of a solid glass bead in water with a single selectively etched hollow tipped fiber probe,[17] and then single fiber OTs came into being.[18,19] So far, structures of single OTs have been developed, such as narrow parabola-like tapered tip fiber OTs,[18] reflection-based fiber-optic tweezers,[20] axicon-tip fiber OTs,[21] high-index fiber-optic tweezers,[22] twin-core fiber OTs,[23] four-core fiber OTs,[24] and others.

For multi-particle trapping research, we can find a relevant report on using the lens OTs,[25] but the difficulty for the lens OTs is that they use the same lens to trap and observe micro-particles, and the trapping direction of the micro-particle is perpendicular to the field of view of the lens: when the first micro-particle is trapped, it will block the second one, third one, and even more, causing inconvenience in practical applications; therefore, relative reports on further research rarely appear. Based on fiber OT technology, whose manipulation view does not depend on the micro-particle trapping direction, Mohanty and Mohanty[26] presented a pair of tapered tip fiber tweezers, which can achieve multi-particle trapping simultaneously, but further research on the trapping principle and characteristics has not been seen until now. However, on the basis of a series of early works above,[25–27] we fabricated a pair of tapered-tip single fiber OTs by a combination of theoretical simulation and experimental verification, which is different from the normal theoretical model simulation method, to analyze the factors influencing the quantity of trapped particles and the trapping characteristics of the single fiber OTs using the finite difference time domain method (FDTD) method, and calibrate the optical trapping force of the single OTs using a pair of calibrated single fiber OTs. These further research results make it feasible to conveniently use the single fiber OTs

*Project supported by the National Natural Science Foundation of China (Grant Nos. 61177081, 61107069, and 61205027), partially supported by the Research Fund for the Doctoral Program of Higher Education of China (Grant No. 20112304110017), the Post-Doctoral Research Fund of Heilongjiang Province, China (Grant No. LBH Q10147), and the Fundamental Research Funds for the Harbin Engineering University of China.

†Corresponding author. E-mail: Drzhihailiu@163.com

© 2014 Chinese Physical Society and IOP Publishing Ltd

in practical researching fields.

2. Fabrication of fiber tapered tip

The normal 980-nm single mode fiber (CL 980 20, NA = 0.2, OFS) with a core diameter of 3.7 μm is employed. A selective chemical etching procedure is employed. The chemical etching solution is composed of 48% hydrofluoric acid (HF), 40% ammonium fluoride (NH_4F), and de-ionized distilled water. The volume ratio of the three solutions is 1.5:1:1.[28] Here we choose 1-bromodecane as the protective liquid layer,[29] which is very important for the final profile of the fiber tip. After 60-min etching in solution at room temperature, the fiber tapered tip has a cone angle of 30°, as shown in Fig. 1.

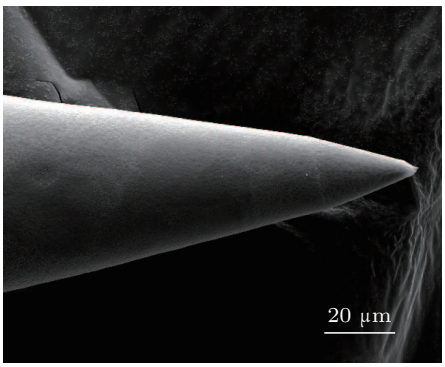


Fig. 1. SEM image of the tapered tip fabricated by the acid etching method.

3. Theoretical analysis of the trapping characteristics

For the tapered tip presented in Fig. 2, it is difficult to obtain an analytical expression for the output light field; therefore, a numerical algorithm such as the FDTD is employed to simulate the output optical field distribution and the optical trapping force of the single fiber OTs.

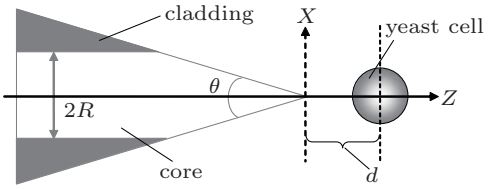


Fig. 2. Schematic diagram of tapered-tip fiber probe. R is the radius of the core; θ is the taper angle. d is the distance between the fiber tip and the micro-particle center.

According to Refs. [18], [30], and [31], the incident wave is two-dimensional (2D). For a TM mode single-frequency continuous wave with components of E_x, E_z, and H_y, the trapping forces are expressed as

$$F_x = \frac{1}{2}\oint_S \left[-\frac{1}{2}(\mu\mu_0 |H_y|^2 + \varepsilon_0\varepsilon_1 |E_z|^2 - \varepsilon_0\varepsilon_1 |E_x|^2)\right] \mathrm{d}z + \oint_S \varepsilon_1\varepsilon_0 \mathrm{Re}(E_x E_z^*)\Big] \mathrm{d}x, \quad (1)$$

$$F_z = \frac{1}{2}\oint_S \left[-\frac{1}{2}(\mu\mu_0 |H_y|^2 + \varepsilon_0\varepsilon_1 |E_x|^2 - \varepsilon_0\varepsilon_1 |E_z|^2)\right] \mathrm{d}x + \oint_S \varepsilon_1\varepsilon_0 \mathrm{Re}(E_x E_z^*)\Big] \mathrm{d}z, \quad (2)$$

where S is the boundary of plane XOZ, ε_0 and ε_1 are the vacuum permittivity and relative permittivity respectively, and μ_0 and μ_1 are the vacuum permeability and relative permeability respectively. From Eqs. (1) and (2), the optical trapping force exerted at boundary S can be obtained fromE_x, E_z, and H_y.

3.1. Trapping the first particle

The output field of the tapered-tip fiber tweezers is simulated and shown in Fig. 3 on the simulation conditions that the cone angle θ is 37°, the fiber core diameter is 3.7 μm, the refractive indices of the core and cladding are 1.46 and 1.45 respectively, the radius and refractive index of the particle are 2.5 μm and 1.40 respectively, and the medium index is 1.33. From Fig. 3 it follows that the divergent field out of the fiber tip is uniform, and the light intensity gradient distribution near the waist is larger than in other places.

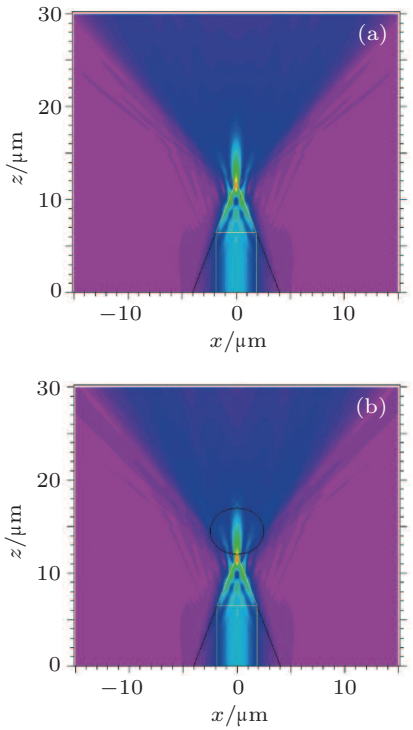


Fig. 3. (color online) Output optical field intensity distributions of probe with taper angle $\theta = 37°$ for the cases (a) without dielectric spheres and (b) with one dielectric sphere with $r = 2.5$ μm and $n = 1.45$.

According to Eq. (1), the calculated values of transverse trapping force (F_x) at different positions ($z = 2.5$ μm, 4.5 μm, and 6.5 μm) along the z axis are presented in Fig. 4; the negative values of the trapping forces indicate that the directions of the forces are along the z axis. The transverse trapping forces

at the origin of the z axis are all zero, which is consistent with the practical situation.

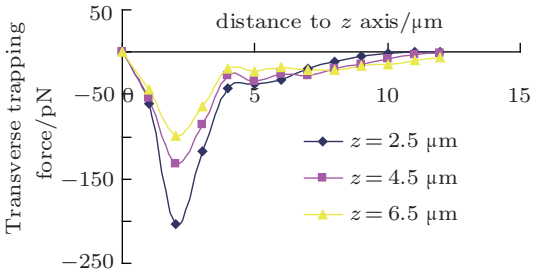


Fig. 4. (color online) Transverse optical trapping force curves at different positions along the z axis.

The axial optical force (F_z) is calculated from Eq. (2). Figure 5 Shows the axial forces exerted on the micro-particles with different refractive indices. The curve of $n = 1.4$, that is generally the refractive index of a biological cell, shows that in a d range of 4 μm–15 μm there is a remarkable negative trapping force, which can pull the particles to the fiber tip.

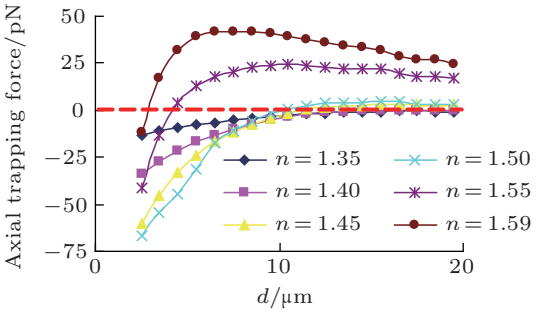


Fig. 5. (color online.) Axial forces of the first particle with different indices. Here the horizontal axis d has been defined in Fig. 2.

Therefore, according to Figs. 4 and 5, the tapered-tip single fiber OTs can trap and manipulate a single dielectric sphere. Besides, we can also predict that the lower the micro-particle refractive index is, the larger the trapping range (trapping force exerted region along the z axis) will be.

3.2. Trapping the second particle

The axial trapping force is the key factor which determines whether the tweezers can trap particles. Therefore we mainly discuss the characteristics of the axial forces. The axial trapping force simulation results for the second particle are shown in Fig. 6. The trapping forces on the second particle with different refractive indices are plotted in Fig. 6 on the assumption that the radii of the first and second particles are the same ($r_1 = r_2 = 2.5$ μm). According to Fig. 6, the second particle is subjected to an axial trapping force when the refractive indices are 1.35, 1.4, and 1.45. The trapping becomes unstable when the refractive index increases to a certain value, such as 1.48. When the refractive index increases to 1.5, the optical forces become larger than zero, which indicates that the fiber tweezers will not be able to trap the second particle. Besides, the trapping range of the tweezers decreases gradually with the particle refractive index increasing from 1.35 to 1.5, which is the same as the property of the first particle.

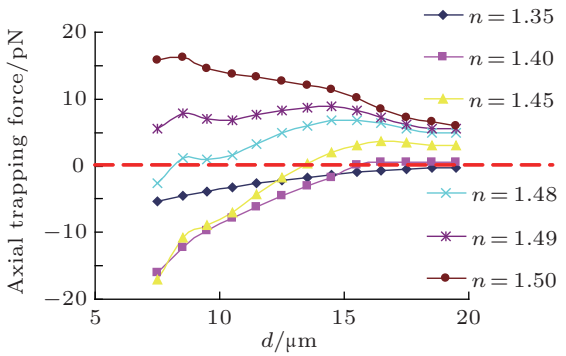


Fig. 6. (color online) Axial forces of the second particle with different indices.

Figure 7 shows that the output optical field is complicated when two particles have been trapped, and the transverse optical trapping force of the second particle ($z = 7.5$ μm) is shown in Fig. 8.

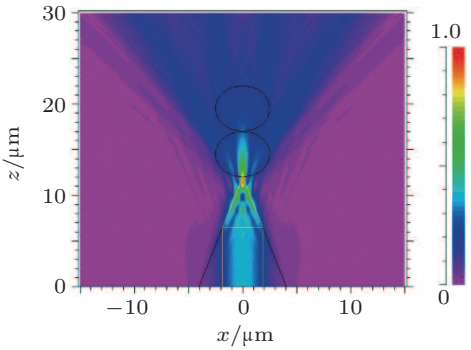


Fig. 7. (color online) Output optical field intensity distribution of the probe with taper angle $\theta = 37°$. The radius and the index of the micro-particle are 2.5 μm and 1.45 respectively.

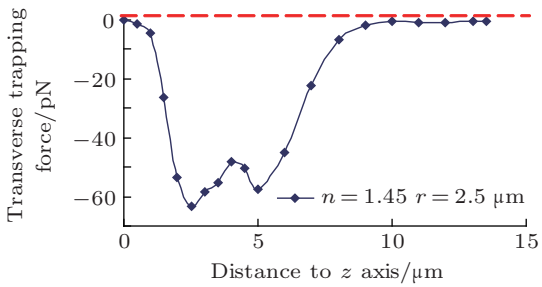


Fig. 8. (color online) Transverse optical trapping force of the second particle. The radius and the index of the micro-particle are 2.5 μm and 1.45 respectively.

3.3. Trapping the third particle

The trapping effect of the OTs on the third particle is also simulated and calculated as shown in Fig. 9, from which there still exist trapping forces when the refractive index of the third particle is less than 1.4; when the refractive index is larger than 1.5, only pushing force is exerted on the third particle.

Compared with the curves of $n = 1.35$ and $n = 1.4$, the trapping range of $n = 1.35$ is much larger than that of $n = 1.4$. Therefore, simulation results indicate that the trapping range of the tapered-tip single fiber OTs is inversely proportional to the refractive index of the trapped particle.

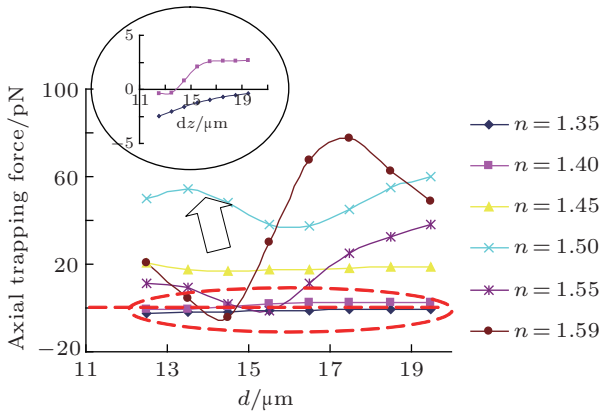


Fig. 9. (color online) Axial forces of the third particle with different indices.

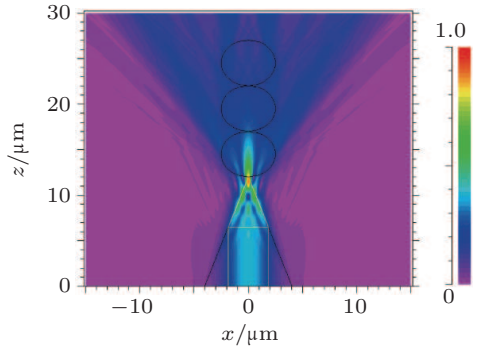


Fig. 10. (color online) Output optical field intensity distribution of probe with taper angle $\theta = 37°$. The radius and the index of the micro-particle are 2.5 μm and 1.45 respectively.

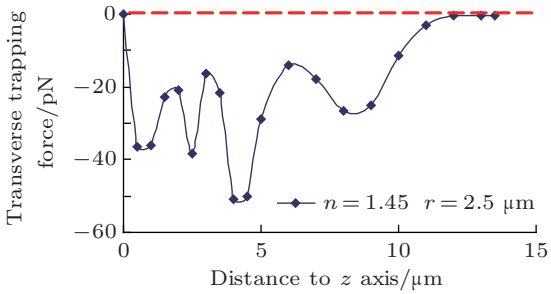


Fig. 11. (color online) Transverse optical trapping force of the third particle. The radius and the index of the micro-particle are 2.5 μm and 1.45 respectively.

Similarly, according to Fig. 10, the output optical field is even more complicated when three particles have been trapped, and the transverse optical trapping force of the third particle ($z = 12.5$ μm) is shown in Fig. 11.

3.4. Trapping multi-particles

Finally, the multi-particle trapping properties are investigated, and the simulation results are shown in Fig. 12, where the strips present the trapping numbers of particles with different radii, and it is apparent that the tweezers can trap multiple particles simultaneously when the refractive index of the particle is small (< 1.5), and the number of the trapped particles decreases quickly with increasing particle refractive index. It can also be seen that the smaller the particle size is, the larger the maximal number of the trapped particles will be. Therefore, we conclude that the refractive index of the dielectric sphere plays an important role in the trapping capability of the tapered-tip single fiber OTs.

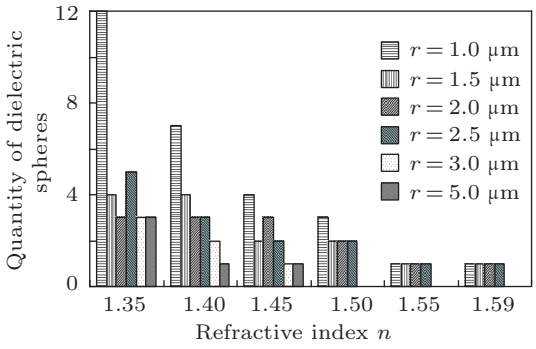


Fig. 12. The numbers of trapped particles with different indices.

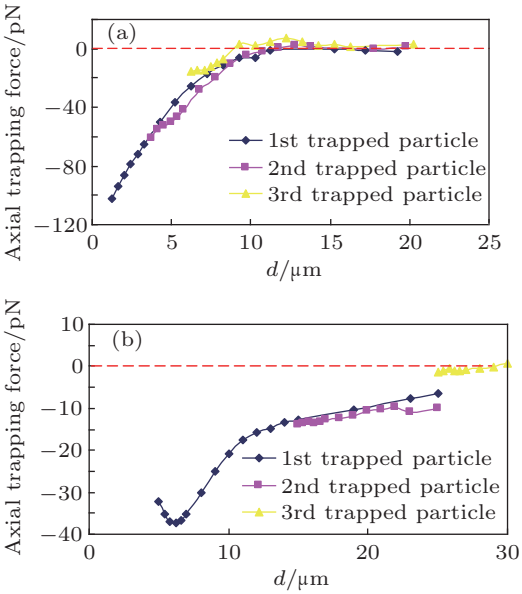


Fig. 13. (color online) Axial optical trapping forces of the yeast cells with the radii of 1 μm (a) and 5 μm (b).

Furthermore, we simulate and calculate the axial optical trapping forces of yeast cells of different sizes, such as $r = 2.5$ μm and $r = 10$ μm. The simulation results are shown in Fig. 13.

4. Experiments

A laser diode (LD) with a wavelength of 980 nm is used as the light source, and the power can be tuned from 0 to 120 mW by adjusting the driving current of the LD. The yeast cells are observed and operated in water with an ordinary reversal optical microscope. The output light power of the OTs is 120 mW. The yeast cells ($r = 2.5$ μm) with a refractive index of ~ 1.4 are chosen as the dielectric spheres.

As shown in Fig. 14, two pairs of single fiber OTs are employed: one is fixed and the other is movable. We use the movable tweezers to trap a cell and then move it to the trapping range of the fixed tweezers; next, we reduce the input optical power of the movable tweezers to release the trapped cell; finally, the released cell is re-trapped by the fixed tweezers.

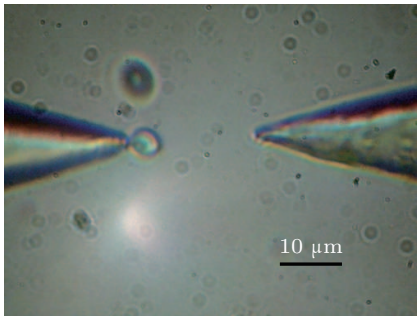


Fig. 14. (color online) Two pairs of tapered-tip fiber OTs transfer one particle.

With this method, we can easily trap one and more cells at the tip of a pair of single tweezers. Photographs of multi-particle trapping are shown in Fig. 15.

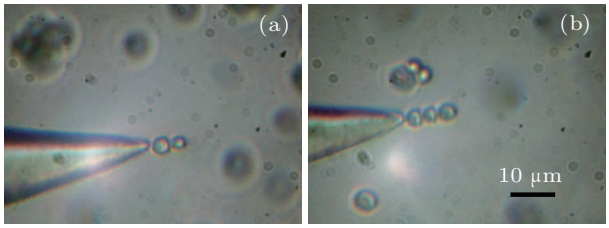


Fig. 15. (color online) Photographs of multi-particle trapping: (a) two particles; (b) three particles.

The trapping force will become smaller when one or more particles have already been trapped, which indicates that the second particle and the third particle will be not easily controlled by the trapping force from this type of tapered-tip single fiber OT. There are also many other factors making the multi-particle trapping unstable. From the simulation curves above, the trapping force is not large when the OTs have trapped more than one particle. The simulation results are consistent with the actual situation.

According to Stokes' law, the output optical power from the movable tweezers versus the trapping force can be calibrated,[17,32] and the results show that when the input optical power increases by 1 mW the trapping force increases by nearly 0.8 pN. Therefore, the calibrated moveable tweezers can not only help the fixed tweezers to trap micro-particles, but also calibrate the fixed tweezers. First, we use the movable tweezers to trap a cell; second, we move the movable tweezers to the trapping area of the fixed tweezers by slowly turning down the power of the laser source. When the fixed tweezers can trap the cell which has been trapped by the movable tweezers, the trapping force from the fixed tweezers and that from the movable tweezers are equal. Therefore, we can realize the calibration of the fixed tweezers, and the relationship between the distance from the tip and the trapping force is shown in Fig. 16. Unfortunately, however, because neither the trapping range nor the trapping force is large enough to trap the third cell, it is hard to calibrate the third cell using this method. The trapping force of the third cell is shown in Fig. 16.

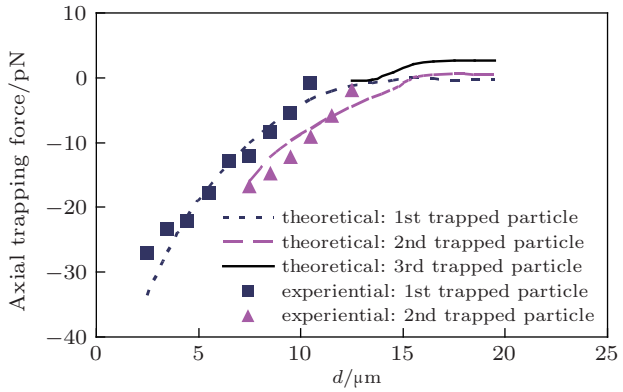


Fig. 16. (color online) Experiential and theoretical results of trapping forces, with different numbers of particles trapped.

The theoretical simulation results of the trapping force are also shown in Fig. 16 on the assumption that the particle index is 1.4 and the radius is 2.5 μm.

Figure 16 shows that the experimental and the theoretical results have the same trends. It is noteworthy that both in the simulation and in the experiment the trapping force of the second particle is larger than that of the first one. The reason may be that the light field is re-focused by the first cell, and the trapping force will be enhanced.

5. Conclusions and discussion

A study of the multi-trapping characteristic of a pair of tapered-tip single fiber OTs is carried out by theoretical and experimental methods. The FDTD method is employed to simulate the trapping characteristic of this pair of fiber OTs, and the results show that the number of trapped particles depends on the refractive index and the size of the particle. Besides, the trapping forces of this pair of tapered-tip single fiber OTs are calibrated by the experimental method, and the results are consistent with the theoretical calculation results. The

multi-trapping function realized by the tapered-tip single fiber OTs will be practical and useful for some applications in the biomedical research field.

There are many factors influencing the experimental results, such as the Brownian motion of the micro-particle, which will offset a part of the optical trapping force, and the simulation model of the OTs, which is ideal and deviates from reality. Therefore, the OTs we use cannot be strictly consistent with the ideal model. These factors cause differences between the experimental results and the simulation results. In the following work, we will investigate the relationship between the trapping force and the factors above, such as the shape, index, and size of the dielectric sphere, the distribution shape and magnitude of the output optical field, and others.

References

[1] Grover S C, Skirtach A G, Gauthier R C and Grover C P 2001 *J. Biomed. Opt.* **6** 14
[2] Haruff H M, Munakata-Marr J and Marr D W M 2003 *J. Colloids. Surf. B* **27** 189
[3] Ashkin A and Dziedzic J M 1987 *Science* **235** 1517
[4] Applegate Jr, Robert W, Squier J, Vestad T, Oakey J and Marr David W M 2004 *J. Opt. Exp.* **12** 4390
[5] Jordan P, Cooper J, McNay G, Docherty F T, Smith W E, Sinclair G and Padgett M J 2004 *J. Opt. Lett.* **29** 2488
[6] Ashkin A, Dziedzic J M, Bjorkholm J E and Chu S 1986 *J. Opt. Lett.* **11** 288
[7] Anderson S E, Younge K C and Raithel G 2011 *Phys. Rev. Lett.* **107** 2630011
[8] Liu C X, Guo H L, Xu C H, Yuan M, Li Z L, Cheng B Y and Zhang D Z 2005 *Chin. Phys. Lett.* **22** 1278
[9] Liu R Q, Yin Y L and Yin J P 2012 *Chin. Phys. B* **21** 033302
[10] Hopkins R J, Mitchem L, Ward A D and Reid J P 2004 *Phys. Chem. Chem. Phys.* **6** 4924
[11] Xu X X, Sarder P, Li Z Y and Nehorai Z Y 2013 *Proc. SPIE* **8615** 86150V
[12] Yao B A and Tassieri A M 2009 *Lab Chip* **9** 2568
[13] Jahnel M, Behrndt M, Jannasch A, Schäffer E and Grill S W 2011 *Opt. Lett.* **36** 1260
[14] Yuan M, Cheng B Y, Zhang D Z, Xu C H, Li Z L, Guo H L and Qu E 2007 *Chin. Phys. Lett.* **24** 2714
[15] Jensen-McMullin C, Lee H P and Lyons E R 2005 *Opt. Express* **13** 2634
[16] Sidick E, Collins S D and Knoesen A 1997 *J. Appl. Opt.* **36** 6423
[17] Taylor R S and Hnatovsky C 2003 *Opt. Express* **11** 2775
[18] Liu Z H, Guo C K, Yang J and Yuan L B 2006 *Opt. Express* **14** 12510
[19] Yuan L B, Liu Z H and Yang J 2007 *Appl. Phys. Lett.* **91** 054101
[20] Bragheri F, Minzioni P, Liberale C, Fabrizio E D and Cristiani I 2005 *J. Opt. Express* **16** 17647
[21] Mohanty S K, Mohanty K S and Berns M W 2008 *J. Biomed. Opt.* **13** 054049
[22] Abedin K S, Kerbage C, Fernandez-Nieves A and Weitz D A 2007 *Appl. Phys. Lett.* **91** 091119
[23] Yuan L B, Liu Z H, Yang J and Guan C Y 2008 *Opt. Express* **16** 4551
[24] Zhang Y, Liu Z H, Yang J and Yuan L B 2012 *J. Lightwave Technol.* **3** 1487
[25] Martin L and Jochen A 2008 *Opt. Commun.* **281** 135
[26] Mohanty K S and Mohanty S K 2007 *Proc. SPIE* **6441** 6441161
[27] Wu X P, Li J, Hu G J, Jun Q, Tao T and Zhang G X 2011 *Acta Phys. Sin.* **60** 030301 (in Chinese)
[28] Chuang Y H, Sun K G, Wang C J, Huang J Y and Pan C L 1998 *Rev. Sci. Instrum.* **69** 437
[29] Hoffmann P, Dutoit B and Salathe R P 1995 *Ultramicroscopy* **61** 165
[30] Gauthier R C 2005 *Opt. Express* **13** 3707
[31] Muller O, Schliwa M and Felgner H 1995 *Appl. Opt.* **34** 977
[32] Gauthier R C and Ashman M 1996 *Appl. Opt.* **37** 6421